

FULLY PLASTIC ANALYSIS OF MIXED MODE
PLANE-STRAIN CRACK PROBLEMS

He Mingyuan (何明元)

Institute of Mechanics, Academia Sinica, China

ABSTRACT

The fully plastic solution for a central crack in an infinite plate subject to a combined loading of mode I and II is given using the modified energy principles. Based on the solution an elastic-plastic mixed mode fracture criterion is suggested. Numerical results for the inclined crack show that the effect of the plastic deformation should be considered in the investigation of the mixed mode fracture criterion. The numerical results for the critical stress are compared with the available experimental data. The agreement is rather good.

THEORETICAL BACKGROUND

The modified energy principles derived in [1] will be used to obtain the fully plastic solution for the combined loading of mode I and II. Let σ^∞ , ϵ^∞ and u^∞ denote the stresses, strains and displacements associated with the uniform field of the loaded body in the absence of the crack. Denote the additional quantities by a tilde so that the total quantities in the presence of a crack are given by

$$\underline{\sigma} = \underline{\sigma}^\infty + \underline{\tilde{\sigma}}, \quad \underline{\epsilon} = \underline{\epsilon}^\infty + \underline{\tilde{\epsilon}}, \quad u = u^\infty + \underline{\tilde{u}} \quad (1)$$

The modified principle of potential energy. If the additional displacements $\underline{\tilde{u}}$ decay faster than $r^{-1/2}$ as $r \rightarrow \infty$, where $r = (x_1^2 + x_2^2)^{1/2}$ among all admissible $\underline{\tilde{u}}$, the exact solutions $\underline{\tilde{u}}$ minimize Φ

$$\Phi(\bar{u}) = \int_V (w(\underline{\varepsilon}) - w(\underline{\varepsilon}^\infty) - \sigma_{ij}^\infty \tilde{\varepsilon}_{ij}) dv - \int_S \sigma_{ij}^\infty n_j \tilde{u}_i ds \quad (2)$$

where v is the infinite region surrounding the crack, s is the crack surface, \bar{n} is the unit normal to s pointing into v , and $w(\underline{\varepsilon})$ is the strain energy density

$$w(\underline{\varepsilon}) = \int_0^{\underline{\varepsilon}} \sigma_{ij} d\varepsilon_{ij} \quad (3)$$

Owing to incompressibility, a stream function could be used to give the additional displacements as

$$\tilde{u}_1 = \psi, \quad \tilde{u}_2 = -\psi, \quad (4)$$

The function is represented as a linear sum of admissible functions in the form

$$\psi = \sum_{i=1}^k A_i \psi^{(i)} \quad (5)$$

The integrals over the body in (2) are evaluated using a mapping technique together with numerical integration in the mapping plane. The physical plane investigated here is mapped into the unit circle in the ζ -plane using the conformal mapping function

$$z = \omega(\zeta) = \frac{a}{2}(\zeta + \zeta^{-1}) \quad (6)$$

where $z = x_1 + ix_2$ and $\zeta = \xi + i\eta = \mu e^{-i\phi}$, as shown in Fig. 2. The polar coordinates μ and ϕ in the mapping plane are taken as the independent variables in the functional representation of ψ .

The numerical results are obtained for the case of a small strain incompressible solid characterized in simple tension by

$$\frac{\varepsilon}{\varepsilon_0} = \alpha \left(\frac{\sigma}{\sigma_0} \right)^n \quad (7)$$

where σ_0 is the yield stress in simple tension, $\varepsilon_0 = E\sigma_0$, and coefficient α and exponent n are material constants. For multiaxial stress states, eq. (7) is generalized to

$$\frac{\varepsilon_{ij}}{\varepsilon_0} = \frac{3}{2} \alpha \left(\frac{\sigma_e}{\sigma_0} \right)^{n-1} s_{ij} \quad (8)$$

where s_{ij} is the stress deviator and σ_e is the effective stress defined by

$$\sigma_e = \left(\frac{3}{2} s_{ij} s_{ij} \right)^{\frac{1}{2}} \quad (9)$$

With an effective strain defined by

$$\varepsilon_e = \left(\frac{2}{3} \varepsilon_{ij} \varepsilon_{ij} \right)^{\frac{1}{2}} \quad (10)$$

σ_e and ε_e satisfy the relation (7). The strain energy density is

$$w(\underline{\varepsilon}) = \int_0^{\underline{\varepsilon}} \sigma_{ij} d\varepsilon_{ij} = \frac{n}{n+1} \alpha \sigma_0 \varepsilon_0 \left(\frac{\varepsilon_e}{\alpha \varepsilon_0} \right)^{\frac{n+1}{n}} \quad (11)$$

FULLY PLASTIC SOLUTIONS

Consider an infinite plate containing a through-the-thickness crack and subjected to a general plane loading, as indicated in Fig. 1. The remote stress components are $\sigma_{22}^\infty = S$, $\sigma_{11}^\infty = T$, $\sigma_{12}^\infty = Q$ and plane strain condition ($\varepsilon_{33} = 0$) is assumed.

For the mode I problem $\sigma_{22}^\infty = S$, $\sigma_{11}^\infty = T$, $\sigma_{12}^\infty = 0$, the stream function suggested in [1,2] is

$$\psi_1(\mu, \phi) = \sum_{k=1}^N \sum_{j=1}^M A_{kj} [\mu^{j-1} \sin 2k\phi + (-1)^{k+1} \cdot 2k(\phi - \frac{\pi}{2})] \quad (12)$$

For the mode II problem, $\sigma_{12}^\infty = Q \neq 0$, $\sigma_{22}^\infty = S = 0$, $\sigma_{11}^\infty = T$ the stream function is taken to be

$$\psi_2(\mu, \phi) = \sum_{k=1}^{N_1} \sum_{j=1}^{M_1} B_{kj} \{ \mu^{j-1} \cos 2(k-1)\phi - (j-1)(-1)^{k+1} \mu^{\frac{1}{2}} [(j-1)(j-2) - 4(k-1)^2] \times \\ (if k=1, j \neq 1,2) \times (-1)^k (\mu^2 - 2\mu) \} \quad (13)$$

This choice is in consistence with the symmetry conditions

$$\psi_2(\mu, \phi) = \psi_2(\mu, -\phi), \quad \psi_{2,\phi}(\mu, \phi) = -\psi_{2,\phi}(\mu, -\phi) \quad (14)$$

and it also ensures that \tilde{u}_1 and \tilde{u}_2 are well behaved near the crack tip.

For $n = 1$, the representation (13) leads to the correct solutions of

u_1 and u_2 as $\mu \rightarrow 1$

For the general case, $S \neq 0$, $Q \neq 0$ and $T \neq 0$, the stream function is taken to be

$$\psi(\mu, \phi) = \psi_1(\mu, \phi) + \psi_2(\mu, \phi) \quad (15)$$

In mixed mode, we use J-integral as a measure of the strength of singularity at the crack tip. The definition of J is the energy release rate when the crack extends along the crack plane. But generally speaking, under the combined loading, the crack will extend not along the crack plane. J-integral is not the true energy release rate. It is only a measure of the strength of singularity. For linear elastic case, J is related to the elastic stress intensity factors by

$$J = \frac{1-\nu^2}{E} (K_I^2 + K_{II}^2) \quad (16)$$

For the infinite plate with crack of length $2a$, the crack length is the only length quantity, and by dimensional considerations J and ϕ_{\min} have the following relation:

$$J = -\frac{1}{a} \phi_{\min} \quad (17)$$

For any admissible additional displacement field \tilde{u} , $\phi(\tilde{u}) \geq \phi_{\min}$, and thus an estimate of J using

$$J = -\frac{1}{a} \phi(\tilde{u}) \quad (18)$$

is necessarily a lower bound. Equation (18) will be used to obtain the numerical estimates of J.

In mixed mode, the parameter M^e , which was introduced in [3] by Shih, is used here. The definition of M^e is

$$M^e = \frac{2}{\pi} \arctan \frac{\sigma_{\theta\theta}^{\infty}(\theta=0)}{\sigma_{\gamma\theta}^{\infty}(\theta=0)} \quad (19)$$

With this definition, M^e ranges from 0 to 1, with $M^e = 0$ for mode II problem and $M^e = 1$ for mode I problem.

The normalized J is given by

$$h(n, M^e) = \frac{J}{\sigma_e^{\infty} \epsilon_e^{\infty} a} \quad (20)$$

where σ_e^{∞} and ϵ_e^{∞} are the remote effective stress and effective strain respectively. Numerical results of $h(n, M^e)$ for $M^e = 0, 0.3, 0.7, 1.0$ and $n = 1, 2, 3, 5, 7, 10$ are given in Table 1 and Fig.3. Because the stream function representation leads to the correct solutions of u_1 and u_2 as $\mu \rightarrow 1$ for $n = 1$, only a few parameters are necessary to give J to the accuracy of three significant figures. The present results for linear elastic case ($n = 1$) were compared with the analytical results, which are also included in Table 1. It was found for all M^e , the difference is less than 0.1%. For $n \neq 1$, on the basis of numerical experimentation with different N, M, N_1 and M_1 , the calculations with $N=3, M=3, N_1=3, M_1=4$ (for $M^e=0.3, 0.7$), $N=0, M=0, N_1=4, M_1=5$ (for $M^e=0$), give results for J in Table 1 which are felt to be lower by an amount less than 5%. As indicated in [1], the upper and lower bounds of J are very close for mode I problem. So it is expected that the numerical results in Table 1 are highly accurate, although here we only calculated the lower bound.

Table 1 $h(n, M^e)$ for plane strain crack

M^e	$n=1$	$n=2$	$n=3$	$n=4$	$n=5$	$n=7$	$n=10$	$n=1^*$
1.0	3.142	4.470	5.511	6.390	7.152	8.421	9.870	3.142
0.7	1.942	2.731	3.291	3.714	4.042	4.508	4.940	1.941
0.3	0.9286	1.314	1.599	1.825	2.006	2.272	2.529	0.9290
0	0.7850	1.120	1.387	1.611	1.804	2.112	2.439	0.7854

* analytical results

Contours for constant effective strain $\epsilon_e = 1.5$, when the remote effective strain is unity, are shown in Fig.4 for different M^e and n . The plots clearly show the strain concentration is relatively smaller in mode II ($M^e=0$) problem and $M^e=0.3$ at a given distance from the crack tip than that in mode I problem, especially for large n . It may explain why materials have a higher fracture toughness in mode II than in mode I.

ELASTIC-PLASTIC MIXED MODE FRACTURE CRITERION

As an engineering approach we assume that in mixed mode the crack will initiate when J-integral approaches its critical value

$$J = J_{cr} \quad (21)$$

We use the estimation scheme proposed by Shih and Hutchinson^[4,5] to calculate the J-integral in the elastic-plastic regime.

$$J = J_e + J_p \quad (22)$$

where J_e is the elastic contribution and J_p is obtained from fully plastic solution.

Now we consider an inclined crack in an infinite plate. The crack makes an angle β to a remote uniform stress σ . Referring to Fig.1 it corresponds to the following loading condition:

$$S = \sigma \sin^2 \beta, \quad Q = \sigma \sin \beta \cos \beta, \quad T = \sigma \cos^2 \beta \quad (23)$$

and $M^e = \frac{2}{\pi} \beta$ (β in radians). The normalized J for the inclined crack is given in Fig.5 for $n=1, 2, 3, 4, 5, 7, 10$. Using the estimation scheme (22) these fully plastic solutions can be used to evaluate the critical stress according to the criterion (21). Let $\sigma_{cr}(\beta)$ denote the critical stress at initiation of crack growth and γ , the stress ratio

$$\gamma = \frac{\sqrt{3} \sigma_{cr}(\frac{\pi}{2})}{2 \sigma_0}$$

The plots of the critical stress ratio $\sigma_{cr}(\beta)/\sigma_{cr}(\frac{\pi}{2})$ versus the crack angle β for $n=3, 10$ and $\gamma=0.4, 0.8$ are shown in Figs.6 and 7. It is assumed that the crack length is the same in all cases. These curves show that the critical stress is dependent on γ , and the effect of plastic deformation should be considered in the investigation of the mixed mode fracture criterion.

Finally, we compare the numerical result of the critical stress with the available experimental data obtained by Xu et al.^[6], and Pook^[7]. The materials used were: LY12-CS aluminium alloy ($\sigma_0=32.5\text{kg/mm}^2, \sigma_u=45.5\text{kg/mm}^2, n=8$) by Xu et al.^[6]; DTD5050 (5½% Zn aluminium alloy, $\sigma_0=34\text{kg/mm}^2, \sigma_u=37\text{kg/mm}^2$) by Pook^[7], the n value for DTD5050 is not given in [7], as it is a fairly ductile material with low work hardening rate, so we use $n=10$ for the calculation. The results are given in Fig.8. The agreement between numerical results and experiment is rather good.

REFERENCES

- [1] He Mingyuan and J. W. Hutchinson, Bounds for Fully Plastic Crack problems for Infinite Bodies, Harvard University Report MECH-22, Oct., (1981), Presented at the second International Symposium on Elastic-Plastic Fracture Mechanics, Philadelphia, 6-9 Oct., (1981), to be published in ASTM STP.
- [2] He Mingyuan and J. W. Hutchinson, J. App. Mech. 48, 830 (1981).
- [3] Shih, C. F. in "Fracture Analysis" ASTM STP 560 187-210 (1974).
- [4] Shih, C. F. in "Mechanics of Crack Growth" ASTM STP 590 3-22 (1976).
- [5] Shih, C. F. and J. W. Hutchinson J. of Eng. Mat. and Tech., Trans of ASME, Series E 98, 289-295 (Oct., 1976).
- [6] Xu Jilin, Xue Yinian and Han Jinhui, An Elastic-Plastic Fracture Investigation On stable Crack Growth For Plane Stress, Report of Institute of Mechanics (Jan., 1983)
- [7] Pook, L. P., Eng. Fract. Mech. 3, 3, 205-218 (Oct., 1971).

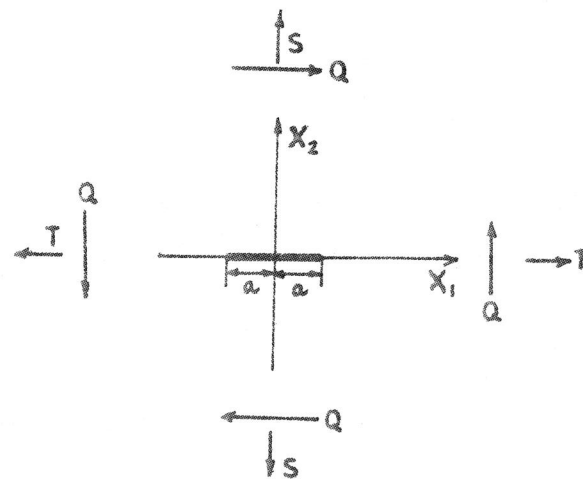


Fig.1 crack geometry

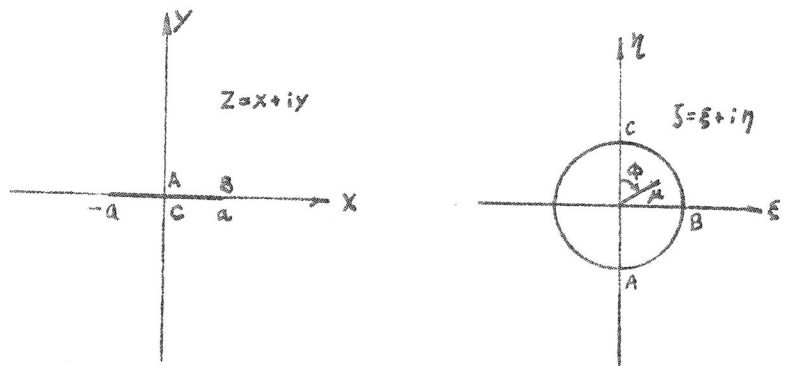


Fig.2 Mapping from physical Plane to mapping plane

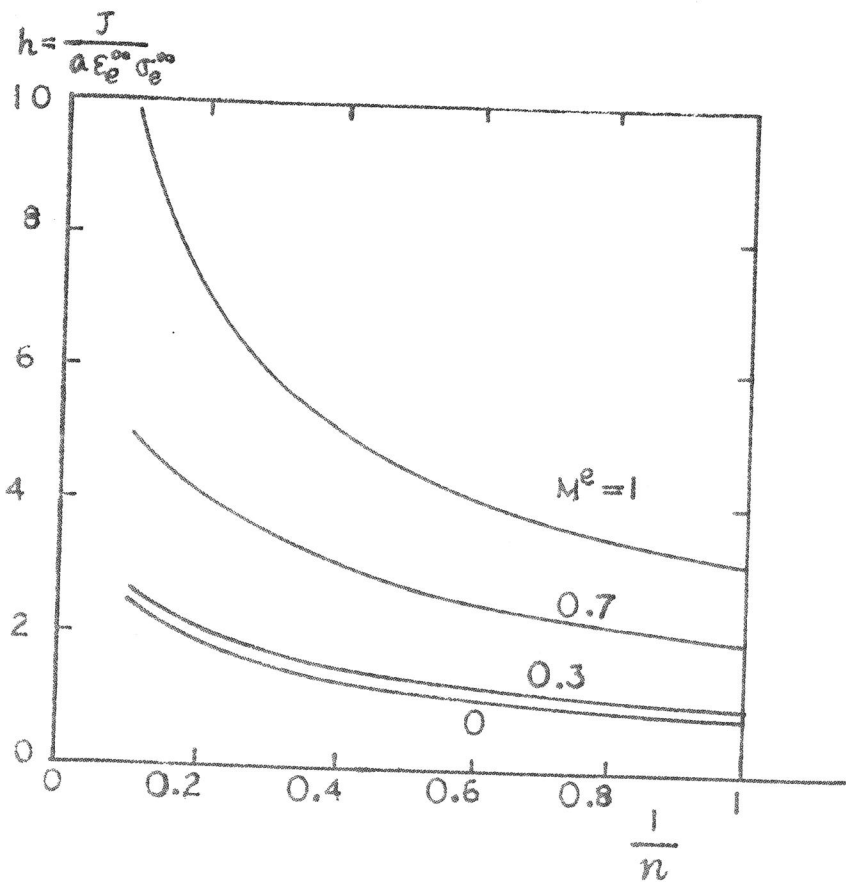


Fig.3 Normalized J for the central crack

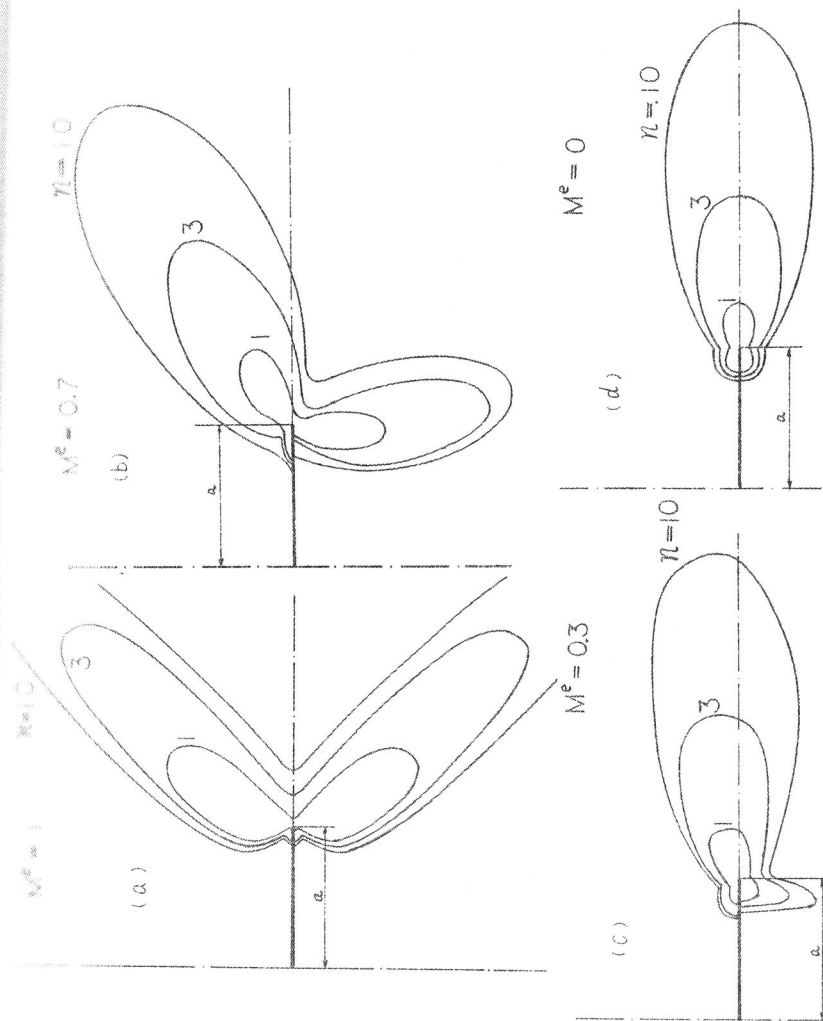


Fig.4 Contours of constant effective strain $\epsilon_e = 1.5$ with $\epsilon_e^{\infty} = 1$. (a) $M^e = 1$ (pure mode I) (b) $M^e = 0.7$ (c) $M^e = 0.3$, (d) $M^e = 0$ (pure mode II)

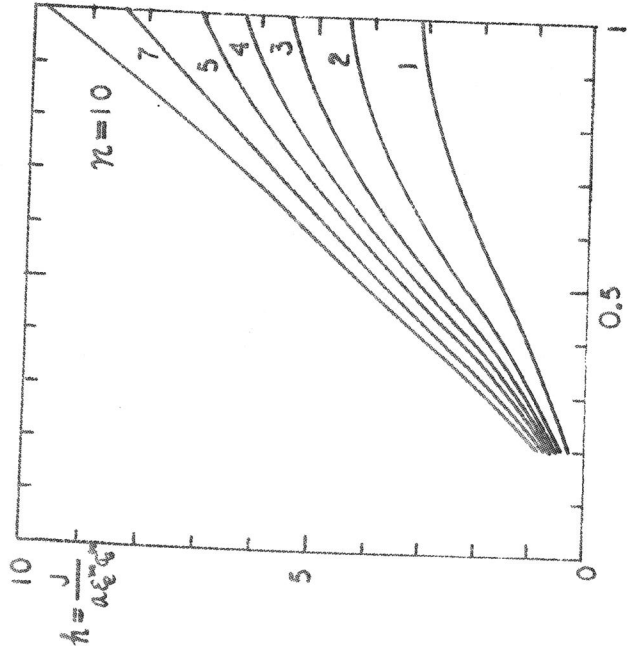


Fig. 5 Normalized J for the inclined crack

$$M^e = \frac{2}{\pi} \beta$$

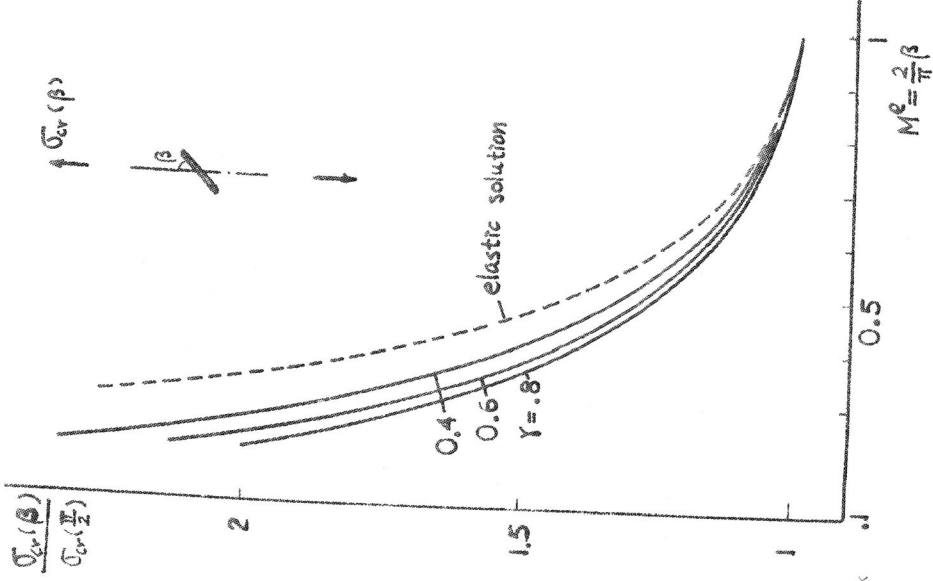


Fig. 6 The critical stress ratio versus the crack angle for $n=3$

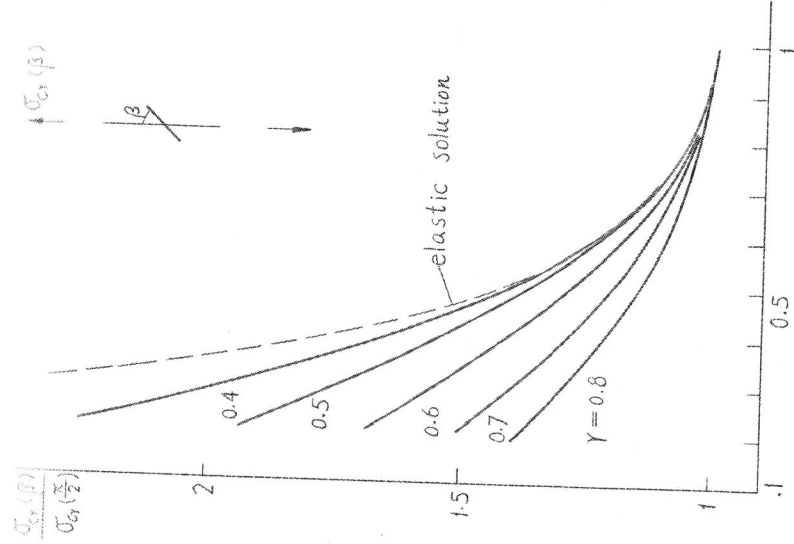


Fig. 7 The critical stress ratio versus the crack angle for $n=10$

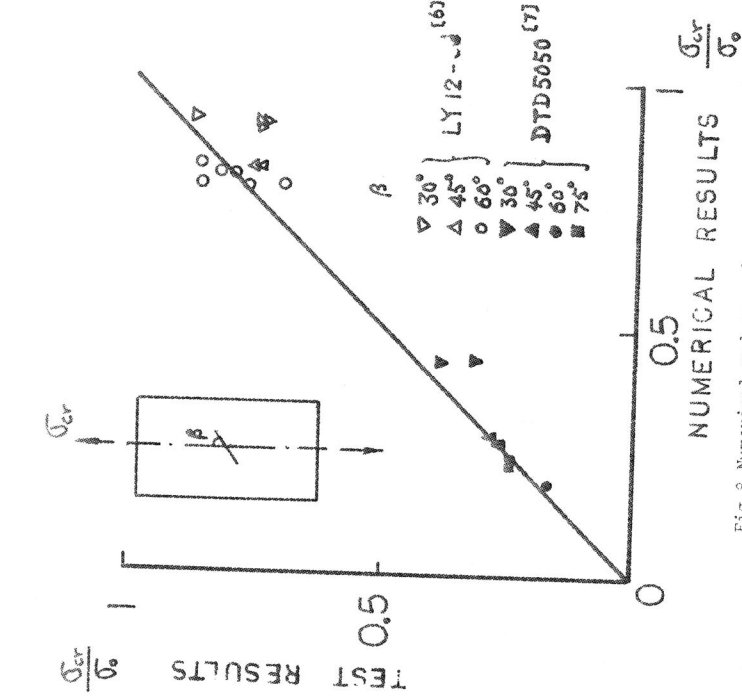


Fig. 8 Numerical and experimental results for the inclined crack

THROUGH-THE-THICKNESS CRACK IN BIAXIAL STRESS FIELD

He Mingyuan (何明元)

Institute of Mechanics, Academia Sinica, China

ABSTRACT

The effects of biaxial stress ratio on the crack tip strain field and J integral have been evaluated numerically for both plane strain and plane stress cases in an infinite body of power-law material using modified energy principles. These fully plastic solutions may also be applied to power-law creep materials. The elastic-plastic solution of J integral for the crack in biaxial stress field was also obtained using the simplified analytical method. Sets of limit curves have been prepared to evaluate the effects of both biaxial stress ratio and applied stress level on J. It is shown that the effect of biaxial stress state on J is negligible below the limit curves. The results are in good agreement with the available fatigue crack propagation data in biaxial fatigue tests.

INTRODUCTION

Fracture mechanics techniques are currently used to predict safe life of aircraft and other structural components. Because multiaxial loading is usually encountered in structural components, it is important to evaluate and quantify multiaxial effects. However, the biaxial stress effect on the crack tip stress field has not been successfully and systematically studied so far, probably because of difficulties in elastic-plastic analysis for various kind of materials.

The purpose of the present investigation is to evaluate systematically the effect of the biaxial stress on the J-integral of a through-the-thickness crack, based on modified energy principle.

FULLY PLASTIC ANALYSIS

Consider an infinite plate, containing a through-the-thickness crack, which is subjected to a biaxial stress field. One of the stress components S is acting perpendicular to the crack and another component T parallel to the crack. Within the context of small strain theory, we consider an incompressible power-law solid characterized in simple tension by

$$\frac{\epsilon}{\epsilon_0} = \alpha \left(\frac{\sigma}{\sigma_0} \right)^n \quad (1)$$

where σ_0 is the yield stress in simple tension $\epsilon_0 = E\sigma_0$, coefficient α and exponent n are material constants. Generalization of Eq. 1 to multiaxial stress state using J_2 deformation theory gives

$$\frac{\epsilon_{ij}}{\epsilon_0} = \frac{3}{2} \alpha \left(\frac{\sigma_e}{\sigma_0} \right)^{n-1} \frac{S_{ij}}{\sigma_0} \quad (2)$$

where S_{ij} and $\sigma_e (= \sqrt{(3/2)S_{ij}S_{ij}})$ are the stress deviator and effective stress, respectively.

The normalized J for plane stress and plane strain are given by

$$h_1(n, T/S) = \frac{J}{\alpha \sigma_0 \epsilon_0 a \left(\frac{S}{\sigma_0} \right)^{n+1}} \quad \text{for plane stress} \quad (3)$$

$$h_2(n, T/S) = \frac{J}{\alpha \sigma_0 \epsilon_0 a \left(\frac{\sqrt{3}S}{2\sigma_0} \right)^{n+1}} \quad \text{for plane strain} \quad (4)$$

h_1 and h_2 are calculated by modified energy principles developed in [1] and [2]. For plane stress case, a stress function is used to generate additional equilibrium stress field. The upper bound of J integral is obtained by modified principle of complementary potential energy. For the plane strain case, a stream function is used to give the additional displacements. The lower bound of J integral is obtained by modified principle of potential energy. These methods have been explained in detail in [2].

Plots of the normalized J versus the biaxial stress ratio T/S are given in Figs. 1 and 2. These curves show the effect of biaxial stress ratio T/S on J integral in fully plastic condition for different n . It is noted that the effects of biaxial stress ratio on J are quite different for the plane strain and plane stress cases.

These solutions are applicable to the situations where the cracked

configurations are completely yielded, i.e., the plastic strains are large enough compared to the elastic strains everywhere in the body. The solution may also be applied to power-law creeping materials under steady-state creep conditions. Most crack problems of practical interest are in the elastic-plastic region, in this range an estimation scheme was used.

ELASTIC-PLASTIC ANALYSIS

The stress-strain relation in simple tension is given by the Ramberg-Osgood formula

$$\frac{\epsilon}{\epsilon_0} = \frac{\sigma}{\sigma_0} + \alpha \left(\frac{\sigma}{\sigma_0} \right)^n \quad (5)$$

An estimation scheme developed by Shih and Hutchinson^[3,4] was used for J. This formula combines the linear elastic and the fully plastic contributions and is of the form

$$J = J_e + J_p \quad (6)$$

where J_e is the elastic contribution which is independent of the component T and J_p is given by fully plastic solution. Formula (6) has been found to be in good agreement with finite element calculations for the complete range of elastic-plastic deformation and material hardening properties for a number of crack configurations^[5].

For the through-the-thickness crack in a biaxial stress field in plane stress case, from (3) and (6), J integral is given by

$$J = J_e + \alpha \sigma_0 \epsilon_0 h_1(n, T/S) \left(\frac{S}{\sigma_0} \right)^{n+1} \quad (7)$$

where $h_1(n, T/S)$ is the normalized J_p of fully plastic solution, which is given in Fig. 1. Then

$$\frac{J}{J_e} = 1 + \frac{\alpha h_1(n, T/S)}{\pi} \left(\frac{S}{\sigma_0} \right)^{n-1} \quad (8)$$

For plane stress case, plots of J/J_e as function of T/S for different S/σ_0 and $n=7, 10$, $\alpha=1$ are given in Fig. 3. Similarly, plots of J/J_e for plane strain case ($n=7$, $\alpha=1$) are given in Fig. 4. These curves show the effects of both biaxial stress ratio S/T and applied stress level s/σ_0 for different

materials.

Finally, for convenience of application, sets of the so called limit curves have been prepared based on J/J_e curves to evaluate the effects of both biaxial stress ratio T/S and applied stress level S/σ_0 on J for plane stress case. It is given in Fig. 5 for $n=7, 8.5$ and 10 . Below the limit curves the effect of biaxial stress state on J is less than 5%, or is negligible from engineering point of view. Above these curves J is affected by stress biaxiality.

The limit curves as shown in Fig. 5 may be used for evaluating the biaxial loading effects on the fatigue crack propagation rate (FCPR) as well as on J. If a set of data ($\Delta S/\sigma_0$, $T/\Delta S$), where ΔS is the range of applied stress S in a fatigue cycle, is located below the limit curve the effect of biaxial stress state on J, then on the FCPR is negligible. The data of tests, conducted by Liu et al.^[6], Joshi et al.^[7] and Truchon et al.^[8], are also included in Fig. 5. The solid points are the data of tests which indicate that the effect of biaxial stress state on the FCPR is negligible. The squares are the data of tests which indicate that the FCPR is affected by biaxial stress state. Most of the solid points are located below the limit curves and all the squares are located above the limit curves. It shows that the experimental data are consistent with the evaluation by the limit curves.

REFERENCES

- [1] He Mingyuan and J. W. Hutchinson, *J. App. Mech.*, 48 (1981), 830.
- [2] He Mingyuan and J. W. Hutchinson, "Bounds for Fully Plastic Crack Problems for Infinite Bodies" Harvard University Report MECH-22, Oct. (1981), Presented at the Second International Symposium on Elastic-Plastic Fracture Mechanics, Philadelphia, 6-9 Oct. (1981), to be published in ASTM STP.
- [3] Shih, C.F., in "Mechanics of Crack Growth" ASTM STP, 590 (1976), 3-22.
- [4] Shih, C.F. and J.W. Hutchinson, *J. of Eng. Mat. and Tech.*, Trans of ASME, Series E 98 (Oct., 1976), 289-295.
- [5] Kumar, V., M.D. German and C.F. Shih, "An Engineering Approach for Elastic-Plastic Fracture Mechanics" EPRI NP-1931 RP1237-1 Topical Report (July 1981).
- [6] Liu, A.F., J.E. Allison, D.F. Dittmer and J.R. Yamane, in "Fracture Mechanics" ASTM STP 677 (1979), 5-22.

- [7] Joshi, S.R. and J. Shewchuk Exp. Mech. 10, 12 (1970), 529.
 [8] Trnchon, M., M. Amestoy and K. Dang-Van, in "Advances in Fracture Research" (ICF 5) 4 (1981), 1841-1849.

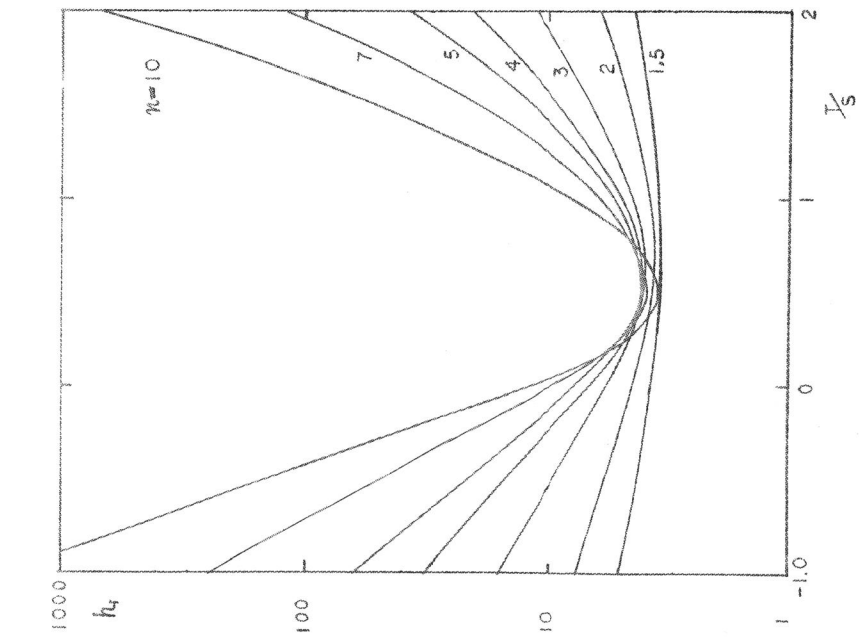


Fig. 1 Normalized J versus T/S for plane stress case (fully plastic solution)

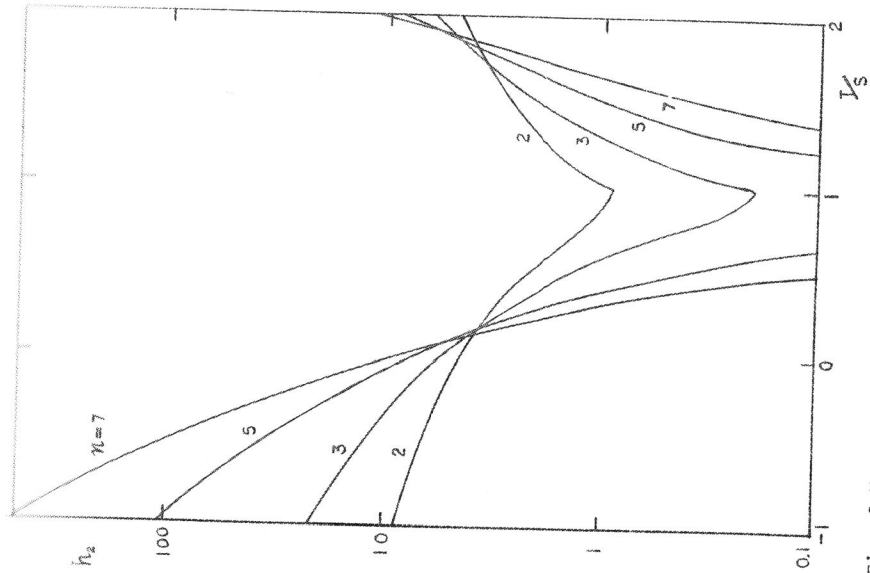
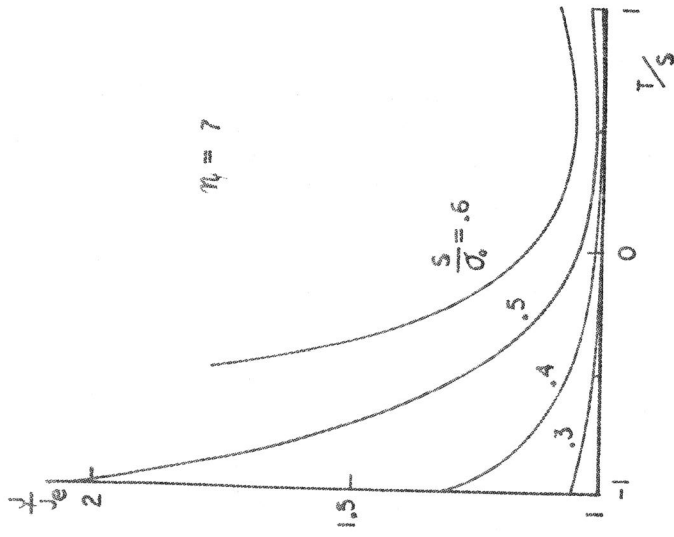
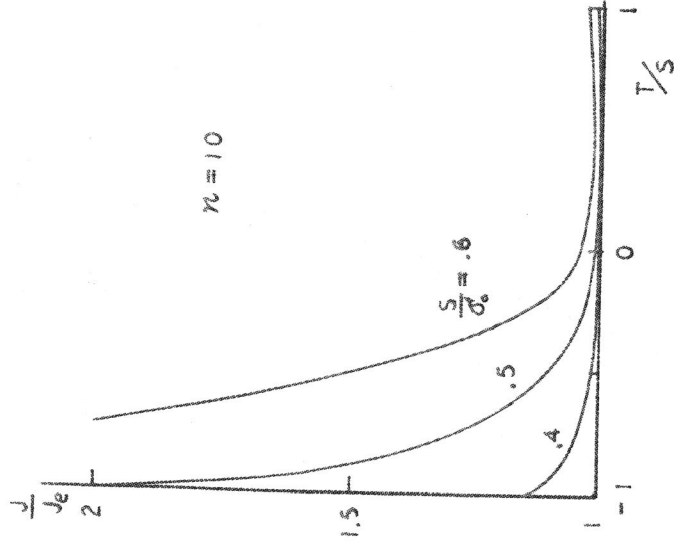


Fig. 2 Normalized J versus T/S for plane strain case (fully plastic solution)

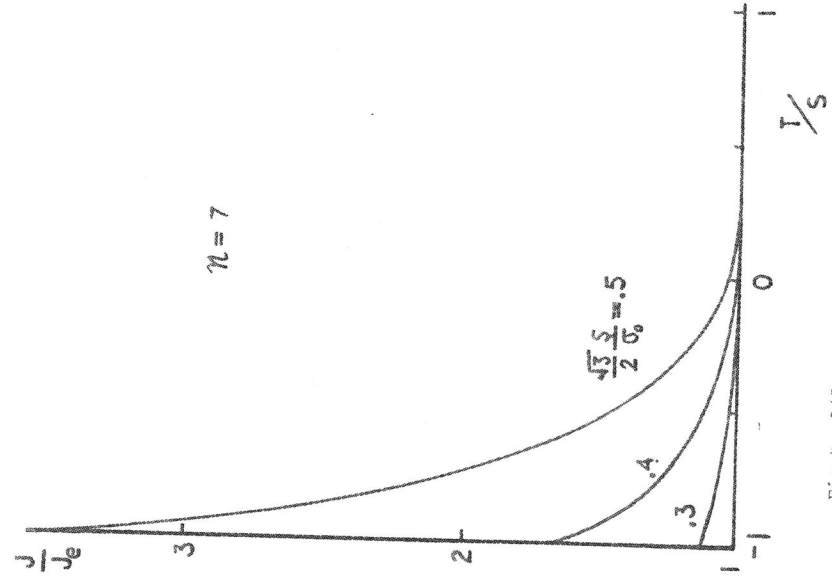


$n = 7$

Fig. 3 J/J_e versus T/S for the plane stress case in different applied stress level (Elastic-Plastic Solutions)(a) $n=7$, (b) $n=10$



$n = 10$



$n = 7$

Fig. 4 J/J versus T/S for the plane strain case in different applied stress level (Elastic-Plastic Solutions) $n=7$

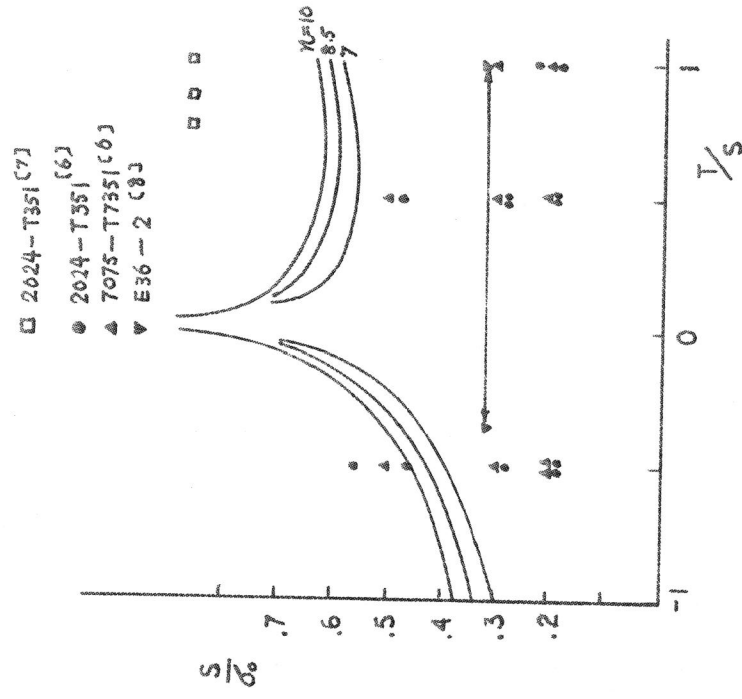


Fig. 5 The limit curves for evaluating the effect of biaxial stress. Experimental results are included